Journal of Analytical and Applied Pyrolysis 173 (2023) 106104

Contents lists available at ScienceDirect

Journal of Analytical and Applied Pyrolysis

journal homepage: www.elsevier.com/locate/jaap

Effect of torrefaction on yield, reactivity and physicochemical properties of pyrolyzed char from three major biomass constituents

Jinzheng Chen [a,b], Zhimin Lu [a,b,*], Jie Jian [c], Zhengyan Bao [a,b], Jianfeng Cai [a,b], Shunchun Yao [a,b,*]

[a] School of Electric Power, South China University of Technology, 510640 Guangzhou, China
[b] Guangdong Province Key Laboratory of Efficient and Clean Energy Utilization, 510640 Guangzhou, China
[c] DTU Chemical Engineering, Technical University of Denmark, DK-2800 Lyngby, Denmark

ARTICLE INFO

Keywords:
Torrefaction
Pyrolysis
Char yield
Reactivity
Physicochemical characteristics

ABSTRACT

Torrefaction is an efficient pretreatment technology for large-scale and high-value utilization of biomass fuel. To understand the effects of torrefaction pretreatment on the physicochemical characteristics of the pyrolyzed char from the three major constituents of lignocellulosic biomass (cellulose, xylan-representative of hemicelluloses, and lignin), torrefied samples were produced at 200, 260, 320, and 380 ℃, and then pyrolyzed at 1028 ℃ with a heating rate of 65 ℃/s and 0.25 ℃/s, respectively. The experimental results demonstrate that the torrefaction temperature strongly influences the pyrolyzed char's yields, oxidative reactivities, and physicochemical structure. The sensitivity of the accumulated char yield and char reactivity to the torrefaction temperature differed with varied constituents. Accurate modeling of accumulated char yield is achieved through a weighted summative law, showing a decreasing deviation from 2.4 wt% to 0.6 wt% as torrefaction temperatures increase. Raman spectra indicate that there is a strong correlation between the relative amount of small and large aromatic rings and the accumulated char yield of torrefied samples, with the determination coefficient R^2 of 0.98, 0.88, and 0.77 for cellulose, xylan, and lignin, respectively.

1. Introduction

Biomass energy is the most promising renewable energy source in the short to medium term [1]. Among the existing technologies to enhance lignocellulosic biomass for clean energy production, torrefaction is a promising pretreatment technique that can significantly improve the fuel property of biomass [2]. Generally, torrefaction means biomass is subject to mild pyrolysis under a temperature of 200–300 ℃ and an oxygen-deficient atmosphere with an appropriate residence time (0.5–2 h) [3]. Torrefied biomass was reported to possess some competitive advantages such as higher energy density, lower moisture content, improved grindability, hydrophobicity, and durability against fungi, which resembles those of low-rank coals and adapts to thermochemical conversion on a large scale [1,4,5]. Compared to the more matured densification pretreatment, torrefaction is still at the research and development demonstration stage [6]. Although the benefits of utilizing torrefied biomass are widely acknowledged in terms of product characteristics, the impact of torrefaction on char formation remains relatively understudied.

Torrefaction alters the physical and chemical properties of the fuel, most noticeably, reduces the volatile contents by half during the most severe torrefactions. As a result, torrefied wood has substantially different pyrolysis behavior than its parent raw counterpart. Char yield is among the most important fuel properties in combustion or gasification, since the conversion of char is the slowest process in most of the boilers and gasifiers.

A simple calculation based on "relative" char yield (equals the weight of pyrolysis char divided by the weight of torrefied sample) data from the literature shows that "relative" char yield influenced by torrefaction in different level increases by a factor of 0.5 [7] to 1.1 [8]. Note that the "relative" char yield will increase just as a result of the moisture and partial volatile release and, thus, mass decrease during torrefaction in the same manner as the inert ash content will do. To ensure an accurate understanding within the context of biomass thermal conversion, it is important to consider the impact of torrefaction on the char yield during the whole torrefaction-pyrolysis process. In this regard, several

* Corresponding authors at: School of Electric Power, South China University of Technology, 510640 Guangzhou, China.
E-mail addresses: zhmlu@scut.edu.cn (Z. Lu), epscyao@scut.edu.cn (S. Yao).

https://doi.org/10.1016/j.jaap.2023.106104
Received 3 July 2023; Received in revised form 25 July 2023; Accepted 28 July 2023
Available online 29 July 2023

terms (equals the weight of pyrolysis char divided by the weight of raw sample), including "absolute" char yield [9,10], "accumulated" char yield[11], "normalized" char yield[7], and "overall" char yield[12], are recommended for assessing pyrolysis char yield. These terms quantify the weight of pyrolysis char in relation to the weight of the raw sample, providing valuable measures for evaluating char yield in the whole thermal conversion process. Ru and Wang [7] found that the "normalized" solid char yield hardly changed as the torrefaction temperature increased from 200 to 300 ℃ (in a TGA), although the "relative" char yield increased up to 29.7%. Insignificant change of the "normalized" solid char yield with increasing torrefaction temperature was also observed in the case of slow pyrolysis conducted in TGA [13,14]. However, Lu et al. [9] found that torrefaction pretreatment of wood increased the "absolute" char yield through a single particle rector (SPR) flame combustion study. Jian et al. [11] experientially demonstrated that torrefaction only had a pronounced impact on the "accumulated" char yield under a high heating rate (> 65 ℃/s) and a high pyrolysis temperature (1028 ℃). Stephen Niksa developed the bio-FLASHCHAIN model to predict the rapid pyrolysis of torrefied biomass [15,16]. He concluded that the reduction in volatiles yields can be attributed to the replacement of bridging within cellulose and lignin macromolecules by added char links. However, as the torrefaction severity increased, the predictions of volatile yield exhibited a growing deviation, ranging from 5 to 10 wt% at a torrefaction temperature of 300 °C. This deviation is significant considering the solid product yields (100 wt% minus volatiles yield). The diversity of experimental results and the inaccuracy of prediction emphasize the need to investigate the char formation characteristics of torrefied biomass in an industrial relevant condition, such as high temperatures and high heating rates.

Numerous studies conducted to date have highlighted the significant influence of torrefaction pretreatment on the reactivity and physicochemical properties of char produced from high temperature and high heating rate. McNamee et al. [17] observed that torrefaction leads to a reduction in reactive structure, consequently decreasing char reactivity. Other researchers have also reported lower char reactivity in torrefied biomass [18,19]. Conversely, Lu et al. [9] found negligible differences in char reactivity with or without torrefaction pretreatment for one hardwood torrefied at 290 ℃ for 1 h. Karlström et al. [20] reported that the char reactivity of torrefied biomass decreases for some materials like olive stones, while it improves or remains the same for straw and pine shells. In terms of char surface morphology, torrefied olive stones were found to exhibit greater porosity compared to raw olive stones [21]. However, contrasting findings were reported by Li et al. [10], who observed that raw char exhibited brittle and porous structures with noticeable openings and fissures in comparison to torrefied char samples. Zhang et al. [22] conducted a study on the physicochemical structure of char derived from torrefied rice husk, revealing that torrefaction led to decreased O/C molar ratios and pore structure in char samples while enhancing aromatization and the ordered degree of the char samples.

In summary, the observed changes in char characteristics, including yield, reactivity, and physicochemical structure, exhibit inconsistent variations with increasing torrefaction temperature, likely due to the variations in feedstock composition and pyrolysis conditions. Consequently, a comprehensive investigation into the fundamental chemical constituents of lignocellulosic biomass, including cellulose, hemicellulose, and lignin, is essential. Such an investigation serves as a benchmark for comparing different biomass types and the effect of various treatments. Although previous studies have investigated the chemical transformation of the three major biomass constituents during torrefaction [23–25] and the impact of torrefaction on the weight loss and distribution of organic fractions in torrefied biomass constituents pyrolysis [26–28], limited attention has been given to the study of pyrolyzed char characteristics. By delving into the char characteristics, we can gain deeper insights into the complex pyrolysis process and further enhance our understanding of the effects of torrefaction on the pyrolysis behavior of biomass constituents.

Our study aims to fill this gap, focusing on the effects of torrefaction pretreatment on the accumulated char yield, reactivity, and structural transformation of pyrolyzed char from the three major biomass constituents. Using a fixed-bed reactor, we consider thermal conditions such as torrefaction temperature and pyrolysis heating rate in the Torrefaction-Pyrolysis two-stage system. The chemical structures of torrefied biomass constituents were characterized by Fourier transform infrared (FTIR) spectroscopy along with nuclear magnetic resonance (NMR), and the physicochemical structure and reactivity of the char samples with different torrefaction pretreatments were accessed by scanning electron microscope (SEM), Raman spectroscopy, and thermogravimetric analyzer.

2. Experimental

2.1. Materials

In this study, three major biomass components were employed, including cellulose, lignin, and model compound xylan, which represented hemicellulose. Cellulose, xylan and lignin were both purchased from Sigma Aldrich. All samples were supplied in fine powder form and no further treatment was applied before the experiment. The proximate and ultimate analysis of the feedstock are given in Table S1 (Supplementary Materials).

2.2. Torrefaction and char preparation

Torrefaction of the three major constituents was conducted in a three-zone electric tube reactor at 200 ℃, 260 ℃, 320 ℃, and 380 ℃ for 60 min (conditions are set identical to a previous study on stepwise pyrolysis of schima wood in the same reactor [11], for the purpose of comparison). In each torrefaction experiment 420 (± 1) mg powder sample was used. Temperature higher than the traditional torrefaction temperature range was employed for a more comprehensive understanding of the influence of torrefaction. For clarity, each torrefaction run was referred to by the first three letters of the material involved, followed by the torrefaction temperature. For instance, Cel-200 (or Xyl-200 and Lig-200) referred to the cellulose (or xylan and lignin) torrefied at 200 ℃. In particular, Cel-Raw, Xyl-Raw, and Lig-Raw were referred to as materials without any pretreatment. The mass yield (Y_m), as an indicator of how biomass resists thermal degradation [10], is defined as Eq. (1):

$$Y_m(\%) = \frac{M_T}{M_R} \times 100\% \quad (1)$$

where M_R and M_T are the sample weights before and after torrefaction, respectively.

Before starting the reaction, ~30 L (STP) of nitrogen was purged into the reactor, and the nitrogen was kept at a flow rate of 1 L/min (STP). The char from the raw constituent was produced by direct pyrolysis. A strategy called stepwise pyrolysis (torrefaction followed by pyrolysis) was used to produce char from torrefied constituents. The first step was low-temperature pyrolysis (i.e., torrefaction) and the second step was high-temperature pyrolysis at 1028 ℃, where the final char was formed. In this article, fast and slow pyrolysis refer to heating rates of ~65 ℃/s and 0.25 ℃/s, respectively. Detailed operational introduction to such a stepwise pyrolysis scheme has been described elsewhere [11]. High-heating-rate char is our primary research focus, because previous research [11] has shown that the reduction in reactivity and promotion in yield of char are more prominent at high heating rate. Low-heating-rate pyrolysis is only discussed for a simple comparison in Section 3.2.2. To distinguish from the "physically concentrated" char fraction because of the decomposition of other unstable fractions during pyrolysis, the "accumulated char yield" (equals pyrolysis char yield

multiplied by torrefaction mass yield) is used to describe the "chemically formed" char. The accumulated char yield (Y_c) is calculated as the char yield on an as-received mass basis, using Eq. (2).

$$Y_c(\%) = \frac{M_P}{M_R} \times 100\% \quad (2)$$

where M_P is the weight of the pyrolyzed char sample.

To compare the difference in the accumulated char yield between the actual biomass (schima wood, studied in a previous study [11]) and the theoretical biomass (computed based on the mass-weighted value derived from the schima wood's fractional composition of the three constituents), the accumulated char yield of the theoretical biomass is obtained using a weighted summative law of the three constituents according to Eq. (3):

$$Y_{c_{TB}} = Cel\% \times Y_{c_{cel}} + Xyl\% \times Y_{c_{xyl}} + Lig\% \times Y_{c_{lig}} \quad (3)$$

where *Cel*%, *Xyl*% and *Lig*% are the percentages of hemicelluloses, cellulose and lignin in the schima wood used in the previous study [11], and $Y_{c_{cel}}$, $Y_{c_{xyl}}$ and $Y_{c_{lig}}$ are the basic constituents' respective individual accumulated char yield with $Y_{c_{TB}}$ is thus the accumulated char yield of the theoretical biomass.

2.3. Thermogravimetric analysis

The oxidation reactivity of the char samples was measured non-isothermally with a thermogravimetric analyzer (TGA, NETZSCH STA 449F5). Approximately 2 mg ground char was heated from 30 ℃ to 120 ℃ for pre-drying and then heated up to 900 ℃ at a heating rate of 10 ℃/min with N_2 and O_2 at flow rates of 95 and 5 mL/min, respectively.

2.4. Characterization of torrefied material by FTIR and ^{13}C NMR

Information about the structural changes of cellulose, xylan and lignin during torrefaction was analyzed by Fourier transform infrared (FTIR) spectroscopy (Nicole, Model iS10). A total of 1 mg of sample was mixed with KBr at a ratio of 1:100 (w/w) and was carefully ground. The FTIR spectra were recorded over the wavenumber range of 400 − 4000 cm^{-1} with a resolution of 4 cm^{-1} for 8 scans. The resultant spectra were normalized to the maximum vibration intensity.

The ^{13}C cross-polarization magic angle spinning (CP/MAS) solid nuclear magnetic resonance (NMR) data was collected at ambient temperature on a Bruker Avance III HD 400 spectrometer at 75.5 MHz. The samples were spun at the magic angle of 90° and at a frequency of 5 kHz. The pulse length and acquisition time were set to be 6 μs and 2 s, respectively.

2.5. Characterization of char by SEM and Raman spectroscopy

Both physical and chemical features of char were investigated. Changes in the surface morphology of raw and torrefied constituents as well as their resultant chars were observed by a field emission SEM (LEO1530VP, Zeiss). The carbon structure transformation of the char samples was characterized by Raman spectroscopy (LabRAM Aramis) at 532 nm laser excitation. The Raman spectra obtained were deconvoluted with the software Peakfit 4.0.

3. Results and discussion

3.1. Characterization of torrefied cellulose, xylan and lignin

3.1.1. Mass yield of torrefied cellulose, xylan and lignin

Fig. 1 shows the mass yields of torrefied cellulose, xylan and lignin with progressive higher torrefaction temperatures. The Y_m of cellulose undergoes a significant reduction in the temperature range from 260 ℃ to 320 ℃, dropping sharply from 84.3% to 17.2%. Xylan is the most reactive among the three major constituents during torrefaction, which loses 27.9% of weight at 200 ℃ and 56.4% at 260 ℃. Unlike cellulose and xylan, lignin thermally degrades over a broad temperature range. The mass yield of torrefied lignin drops from 83.1% to 59.5%, with the torrefaction temperature increasing from 200 ℃ to 380 ℃. Yang et al. [29] reported that lignin is the most difficult one to decompose among the three major constituents, with slow degradation under the temperature range from ambient to 900 ℃. The broad degradation temperature range of lignin is attributed to the various kinds of oxygen-containing functional groups (e.g., phenols, methoxyls, aliphatic alcohols, carbonyls and ethers) and the different thermal stabilities these oxygen-containing functional groups have [30].

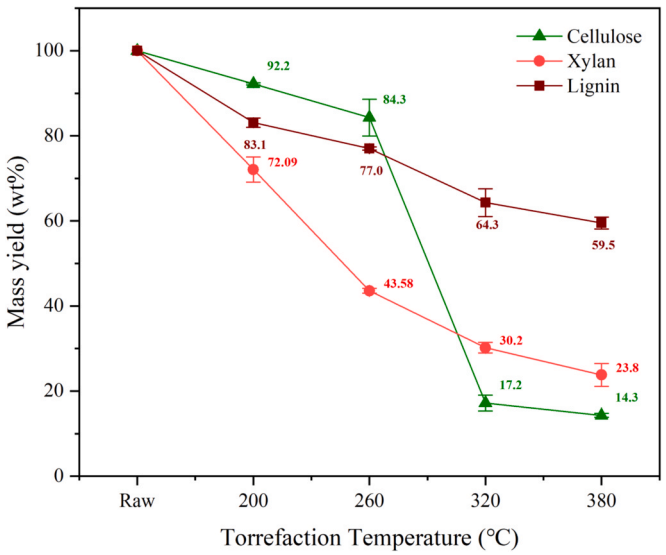

Fig. 1. Mass yields of the three major constituents as a function of torrefaction temperature.

3.1.2. Chemical structure evolution in torrefaction

FTIR (Fig. 2) and ^{13}C NMR (Fig. 3) were employed to estimate the chemical structure evolution of the three major constituents upon torrefaction. Fig. 2a shows the FTIR spectra of torrefied cellulose with varying severity. The spectrum of Cel-200 and Cel-260 is broadly similar to that of Cel-Raw, since the remarkable degradation of organic groups is reported to begin until 280 ℃ [30]. Significant chemical structure change of cellulose is observed for sample Cel-320. The peak at 1634 cm^{-1}, characteristic of C═C absorption in samples pretreated below 260 ℃, splits into two peaks at 1709 cm^{-1} and 1602 cm^{-1} for sample Cel-320, indicative of conjugated C═O and C═C-C═C bonds, respectively [31]. These results reveal that cleavage and rearrangement prevail at 320 ℃ [30]. A decrease in the intensity of peak for -OH (3400–3200 cm^{-1}) also means that cellulose undergoes dehydration and condensation reactions [32].

Fig. 2b shows the FTIR spectra of torrefied xylan with varying severity. The intensity of the C═O (1704 cm^{-1}) absorption peak increases at 200 ℃, indicating the dehydration of the hydroxyl group in the pyran ring and the formation of compounds (furans, aldehydes or ketones) [33,34]. With the increase of the torrefaction temperature (≥ 260 ℃), the typical absorption peaks of xylan at 896 cm^{-1} (C-H deformation), 1045 cm^{-1} (C═O stretching) and 1168 cm^{-1} (C-O-C, β-glucosidic linkage stretching) almost disappear, while the peak at 1630 cm^{-1} associated with the carbonyl stretching conjugate with aromatic rings is still retained. This suggests the significant cleavage of the main chain in xylan (β-1,4–glycosidic bonds) and the occurrence of polycondensation reactions [33,35].

As for lignin, as shown in Fig. 2c, the prominent characteristic peaks

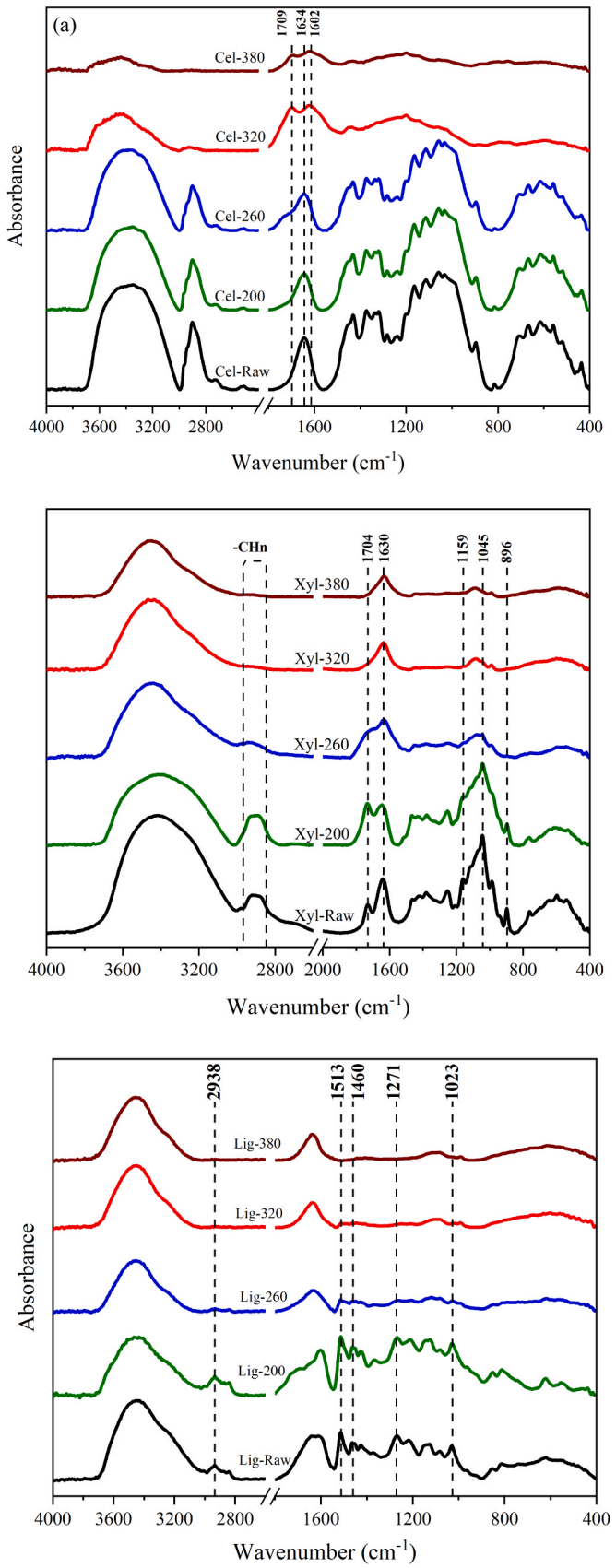

Fig. 2. FTIR spectra of raw and torrefied three major constituents under different torrefaction temperatures (200 ℃, 260 ℃, 320 ℃ and 380 ℃), (a) cellulose, (b) xylan, (c) lignin.

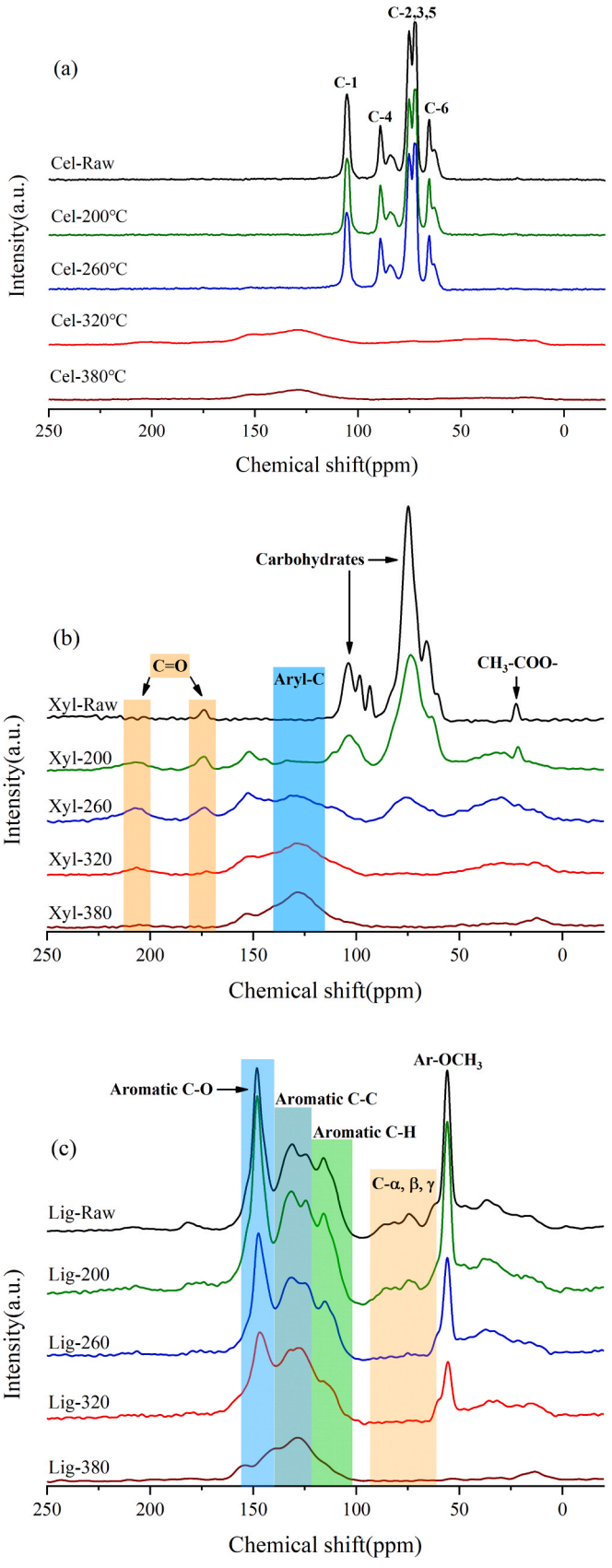

Fig. 3. ^{13}C NMR spectra of the three major constituents and their counterpart pretreated at different temperatures (200 ℃, 260 ℃, 320 ℃ and 380 ℃), (a) cellulose, (b) xylan, (c) lignin.

of lignin are observed to be aliphatic C–H (2938 cm^{-1}), aromatic skeletal vibrations (1513 cm^{-1}), C-H asymmetric deformations and CH_3O- (1460 cm^{-1}), guaiacyl ring breathing with C-O stretching (1271 cm^{-1}) and aromatic C-H in-plane deformation (1023 cm^{-1}) [28,36,37]. These characteristic peaks are drastically diminished at 260 °C, indicating apparent cleavage of β-O-4 bonds and demethoxylation and polycondensation of lignin via aromatic electrophilic substitutions of aromatic nuclei during torrefaction [28]. In contrast to the significant variation of peaks in the wavenumber range from 3000 to 800 cm^{-1}, the wavenumber range from 3700 to 3200 cm^{-1}, indicating the absorption of O-H and C-H stretching vibrations, only has a subtle change.

Fig. 3 presents the solid-state 13 C NMR spectra, allowing for a comparison of the chemical structure evolution between the three major biomass constituents and their torrefied counterparts. The spectra reveal that significant changes occurred. In the case of cellulose and xylan, the carbohydrates undergo substantial decomposition at temperatures of 320 °C and 260 °C, respectively. This is evident from the disappearance of signals (60–110 ppm for cellulose and 50–110 ppm for xylan) in the corresponding NMR curves. The total carbohydrate carbon intensity gradually decreases, suggesting severe crosslinking and charring of cellulose and xylan during torrefaction [19]. Notably, the decomposition of cellulose and xylan coincides with noticeable aromatization. The solid-state 13 C NMR spectra of lignin at different pretreatment temperatures are presented in Fig. 3c. In the chemical shift range of 155–102 ppm, which corresponds to the aromatic region, three subregions can be distinguished: protonated aromatics (δ 123–102 ppm), condensed aromatics (δ 140–123 ppm), and oxygenated aromatics (δ 155–140 ppm) [38]. As the torrefaction temperature increases, there is a significant decrease in protonated and oxygenated aromatic signals, resulting in a higher concentration of condensed aromatic carbons per aromatic ring. This indicates an increased degree of condensation. Additionally, in the aliphatic region (60–90 ppm), the signals corresponding to α, β, and γ carbons weaken with higher torrefaction severity. This suggests a high degree of depolymerization caused by the cleavage of aryl-ether bonds [39].

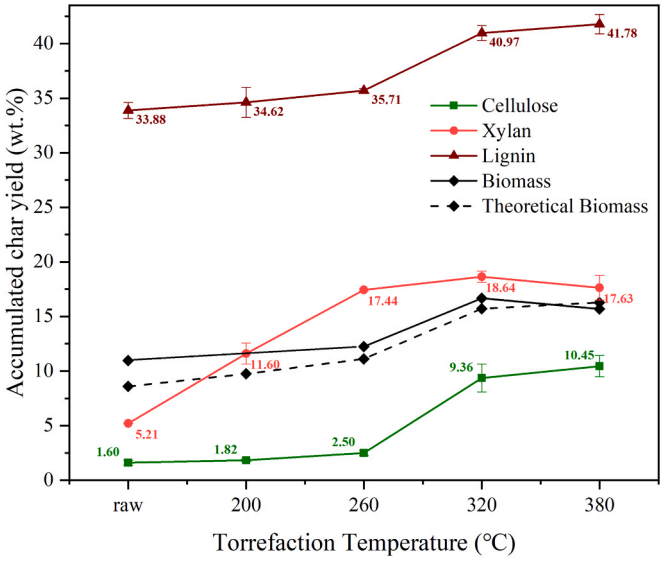

Fig. 4. Accumulated char yields (1028 ℃, 20 min) of the three major biomass constituents torrefied at different temperatures, along with the data from biomass studied at the identical experimental setup under the same condition [11]. The char yield of the theoretical biomass indicates the mass-weighted value based on its fractional composition of the three constituents and their char yield determined in the present study.

3.2. Accumulated char yield

3.2.1. Impact of torrefaction temperature

As seen in Fig. 4, the accumulated char yields Y_c of the untreated three major constituents are 1.60 wt%, 5.21 wt% and 33.88 wt%, respectively, for cellulose, xylan and lignin. The Y_c value for cellulose and lignin shows the same trend with increasing torrefaction temperature that it starts to rise at torrefaction temperatures of 260 ℃ and peaks at 380 ℃, demonstrating a respective 7.90 wt% and 6.07 wt% increment. Regarding xylan, the Y_c increases as the torrefaction severity enhances from raw to 320 ℃, with the highest yield of 18.64 wt% at 320 ℃. However, at 380 ℃, the Y_c of xylan declines slightly to 17.63 wt %. Among the three major constituents, lignin produces the most char and cellulose the least, with xylan in between, which is in agreement with expectation. With torrefaction, the accumulated char yield of these torrefied constituents can be from 1.23 times (for lignin) to 6.53 times (for cellulose) higher than their raw samples.

Fig. 4 also compares the calculated Y_c using the three biomass constituents fractions of a real biomass (Schima wood) with its experimental value. The calculated curve fits the experimental curve well, and the deviation decreases from 2.38 wt% to 0.58 wt% with the progressive higher torrefaction temperatures. The largest difference between the calculated and experimental accumulated char yield in the raw biomass can be attributed to the interaction among the three major constituents during pyrolysis, such as the interaction of levoglucosan released by cellulose with the pyrolysis products of xylan and lignin [40]. The deviation in the predicted char yield can also be attributed to the presence of alkali metals when using the weight fraction additivity law [21]. Furthermore, the incorporation of ash effects resulted in a notable improvement in the model's correlation constant [41]. The accumulated char yield can be modelled accurately using a non-interaction assumption when biomass is torrefied to a certain extent. The reason for the well prediction might be that the torrefaction homogenizes the chemical structure of different biomass constituents, thereby weakening the interactions among them during pyrolysis.

In Fig. 4, the phenomenal growth in Y_c after torrefaction pretreatment exhibits different temperature dependencies for each constituent. Interestingly, the accumulated char yield Y_c exhibits a corresponding trend as the mass yield Y_m (shown in Fig. 1) versus torrefaction temperature. To be more specific, the Y_c and Y_m of cellulose begin to soar or drop respectively above 260 ℃, and those of xylan rise and fall dramatically when torrefied at 200 ℃ and level off above 260 ℃. Regrading lignin, both the Y_c and Y_m gradually increase or decrease with increasing torrefaction temperature. Such correspondence suggests that the phenomenal growth in Y_c was probably induced by the chemical structure transformation occurred in the torrefaction. Hence, an attempt was made to correlate the Y_c with the Y_m; three correlations for three biomass constituents are shown in Fig. 5. Clear linear correlation can be found for all three constituents, where the coefficients of determination are 0.99 for cellulose, 0.96 for xylan and 0.85 for lignin, respectively. In a previous study [10], the authors have correlated the high temperature char yield produced in a flame reactor with the torrefaction mass yield, for wood particle either experiencing oxidative torrefaction or traditional torrefaction. The coefficients of determination for the accumulated char yield are as high as 0.83 and 0.96, respectively, demonstrating the effectiveness using torrefaction mass yield as the indicator.

3.2.2. Impact of pyrolysis heating rate

In Fig. 6, we compare the influence of torrefaction on accumulated char yield under high and low heating rates (65 ℃/s versus 0.25 ℃/s). In the case of slow pyrolysis (0.25 ℃/s), the differences in char yields between the three biomass constituents with and without torrefaction were insignificant, being all within range of experimental uncertainty. However, the results from fast pyrolysis experiments revealed significant differences in char yields. For raw cellulose, xylan, and lignin, the

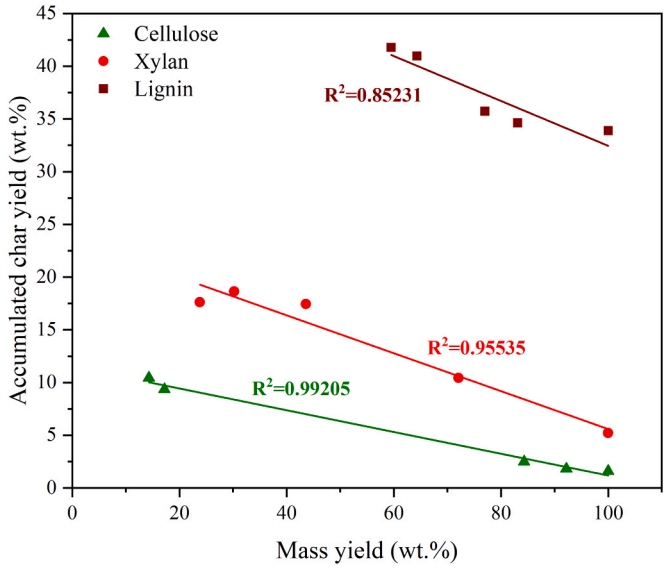

Fig. 5. The accumulated char yield as a function of the torrefaction mass yield for the three major biomass constituents.

char yields were found to be 1.6 wt%, 5.2 wt%, and 33.9 wt%, respectively. In contrast, their torrefied counterparts (320 ℃, 60 min) exhibited significantly higher char yields of 9.4 wt%, 18.6 wt%, and 41.0 wt%, representing a growth factor of 5.9, 3.6, and 1.2 times, respectively. In other words, torrefaction only had an impact on char yield in high heating rates pyrolysis. This phenomenon aligns with the findings of our previous study on raw and torrefied biomass pyrolysis [11], and also is in line with the discoveries in the slow heating TGA experiments [7,13,14]. When comparing separately from slow and fast pyrolysis, the char yield behaviors of the biomass constituents and the previously studied woody biomass with no torrefaction [11] fit the expectation that fast pyrolysis reduces the char yield. Interestingly, it seems that the effect of torrefaction on the fast pyrolysis is to restore the char yield to the level of the slow pyrolysis, as suggested as the dotted line in Fig. 6.

3.3. Char reactivity

The char reactivity of raw and torrefied three major constituents towards oxygen was investigated in a TG instrument to understand the effect of lignocellulosic constituents type and torrefaction temperature. The weight loss signals of the char in 5% volume fraction O_2 are shown as a function of temperature in Fig. 7. The reactivities of varied chars are distinguished and ranked by the positions of those non-isothermal conversion curves, where the temperature at a 50% conversion is defined as the char reactivity index (i.e., T_{50}). Higher T_{50} means poorer reactivity as it requires a higher temperature to reach 50% conversion. The reactivities of the three constituents char exhibit varying trends as torrefaction temperature increases. Based on T_{50} values, the cellulose char reactivity sequence is as follows: Cel-200 char > Cel-Raw char > Cel-260 char > Cel-380 char > Cel-320 char, with a maximum T_{50} difference of 101 ℃. The T_{50} of xylan char oxidation increases by 54 ℃ as torrefaction severity rises from raw to 380 ℃. Regarding lignin, the reactivity can either increase or remain unaffected by torrefaction, as Lig-260 char and Lig-380 char exhibit lower T_{50} values, and the conversion curves for Lig-Raw char, Lig-200 char, and Lig-320 char overlap in the figure, within a narrow T_{50} range of 4 ℃.

To sum up, only the char reactivity of Xylan was reduced by torrefaction pretreatment in a consistent way: T_{50} increased successively with progressively higher torrefaction temperature, with a difference (from 18 to 54 ℃) much higher than the experimental uncertainty, which we estimated to be within 10–20 ℃ from the present study and from our experiences. As to cellulose, torrefaction at 200 ℃ first decreased T_{50} and then raised it to the summit when torrefaction temperature increased to 320 ℃. The reactivity of lignin char exhibited an intriguing trend with increasing torrefaction severity: the T50 value decreased with higher pretreatment temperatures, although not consistently in a linear manner. The char reactivity appears to be intricately influenced by the interplay between the original chemical structures of biopolymers and the physicochemical transformations occurring during torrefaction and pyrolysis. This complexity accounts for the diverse variations in reactivity observed among different biomass constituents char, offering an explanation for the varied observations of char reactivity changes under different torrefaction and pyrolysis conditions for different biomass types. Previous studies using actual biomass have consistently reported that torrefaction reduces char reactivity [11,42,43]. This

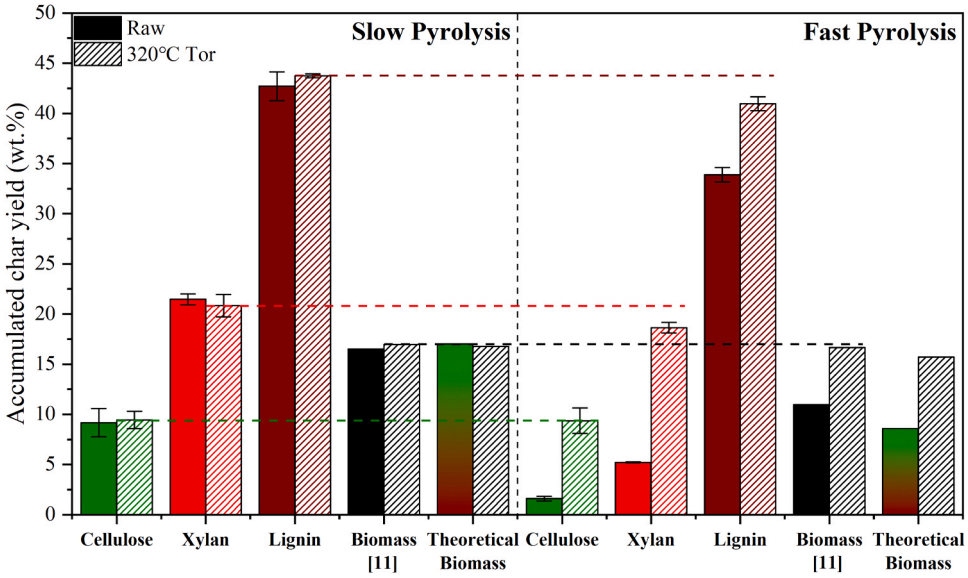

Fig. 6. Accumulated char yields of raw and torrefied (320 ℃, 60 min) constituents in (left) slow pyrolysis (0.25 ℃/s); (right) fast pyrolysis (65 ℃/s), along with the data from biomass studied at the identical experimental setup [11]. The accumulated char yield of the theoretical biomass is calculated from the fractions of the three constituents and their accumulated char yield determined in the present study under the same condition.

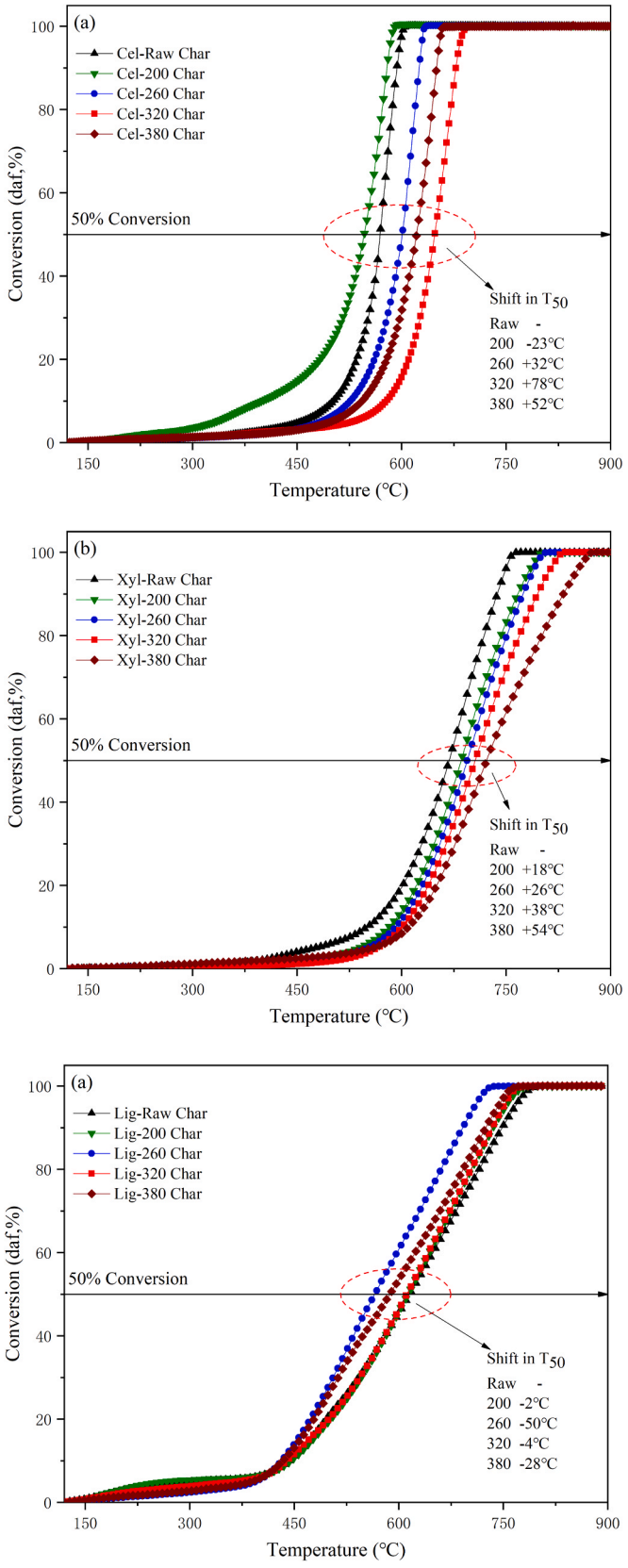

Fig. 7. Non-isothermal TGA conversion curves of pyrolyzed char samples from raw and torrefied three major constituents, (a) cellulose, (b) xylan, (c) lignin. TGA condition: from a pre-dried state of 120–900 °C at a heating rate of 10 °C/min with N_2 and O_2 at flow rates of 95 and 5 mL/min, respectively.

reduction is primarily attributed to factors such as decreased specific surface area, pore volume, and active sites resulting from thermal deactivation. However, there have also been observations of increased char reactivity in torrefied biomass, which can be attributed to the influence of various competing processes during pyrolysis [20] and the higher concentration of AAEMs in the torrefied biomass char [44]. To date, there is a significant gap in the existing literature regarding the char reactivity of torrefied biomass constituents. Further investigations are needed to gain a comprehensive understanding of the impact of torrefaction on the char reactivity of biomass constituents, as well as to unveil the precise role of these constituents in determining the char reactivity of natural biomass.

3.4. Char surface characteristics

Fig. 8 shows the microstructures of parent constituents and their chars. In Fig. 8A&G, raw cellulose and its char present a fiber-like exterior, as the particles are of twisted and oblong shape. Pore is hardly observed on char even though cellulose is abundant in volatiles. When torrefaction is applied, similar features are as well seen. This observation indicates that while the external surface experiences melting during pyrolysis, the crystalline structure of the internal fibrils retains its rigidity [45]. Furthermore, the formation of intermediate molten phases contributes to increased density, thereby impeding the mass transfer of volatile compounds [46]. Comparatively, xylan samples have experienced more considerable change in morphology after torrefaction. According to Fig. 8C&D, particles of raw xylan are tube-shaped with small spheres inside, which is difficult to define, but they change tremendously into flaky shapes as torrefaction is applied. This evident morphological transformation may be due to the low melting point of xylan, which enabled it to transform substantially in torrefaction. Whether torrefied or not, xylan chars are made up of flaky particles. However, the surface of char from torrefied xylan is much smoother than that from raw xylan. Raw-xylan char is porous, while little pore was found on torrefied-xylan char. Fig. 8E shows the raw lignin particles are large lumpy masses. After torrefaction, these large lumps break into small lumps suggesting the depolymerization and formation of smaller units. The performances of raw and torrefied lignin in subsequent high-temperature pyrolysis are significantly different. During pyrolysis, while lumpy particles of raw lignin break into small pellets with a lot of pores on them, those lumpy particles of torrefied lignin are retained.

3.5. Char carbon structure

In order to understand the influence of torrefaction on accumulated char yield by the carbon structure, Raman spectroscopy was employed. An example of Raman spectroscopy is presented in Fig. 9. Different deconvolution methods [47–49] were tested to analyze the spectroscopy further. Considering the preconditions of deconvolution methods, the 10 bands method proposed by Smith et al.[49] is chosen, which has been applied to proposed, and discussed in-depth, and the descriptions of each band are summarized in Table S2 (Supplementary Materials).

In this study, two major bands are discussed to track the evolution of the carbon skeletal structure of the char during pyrolysis. The D band assigns to larger aromatic ring systems and the Ds band stands for smaller aromatic ring systems [45,49]. Thus, the relative amount of small and large rings in the pyrolysis char is evidently reflected by the band area ratio between D and Ds. The band area ratio A_D/A_{Ds} for char with different torrefaction severity is determined and plotted in Fig. 10, versus corresponding accumulated char yield. As displayed in Fig. 10, the band ratio A_D/A_{Ds} increases with increasing accumulated char yield as torrefaction severity deepens. With increasing torrefaction severity, the band ratio A_D/A_{Ds} for cellulose char, xylan char and lignin char are increasing from 1.26 to 2.65, from 1.08 to 1.61 and from 1.14 to 1.35, respectively, implying that torrefaction promote polycondensation

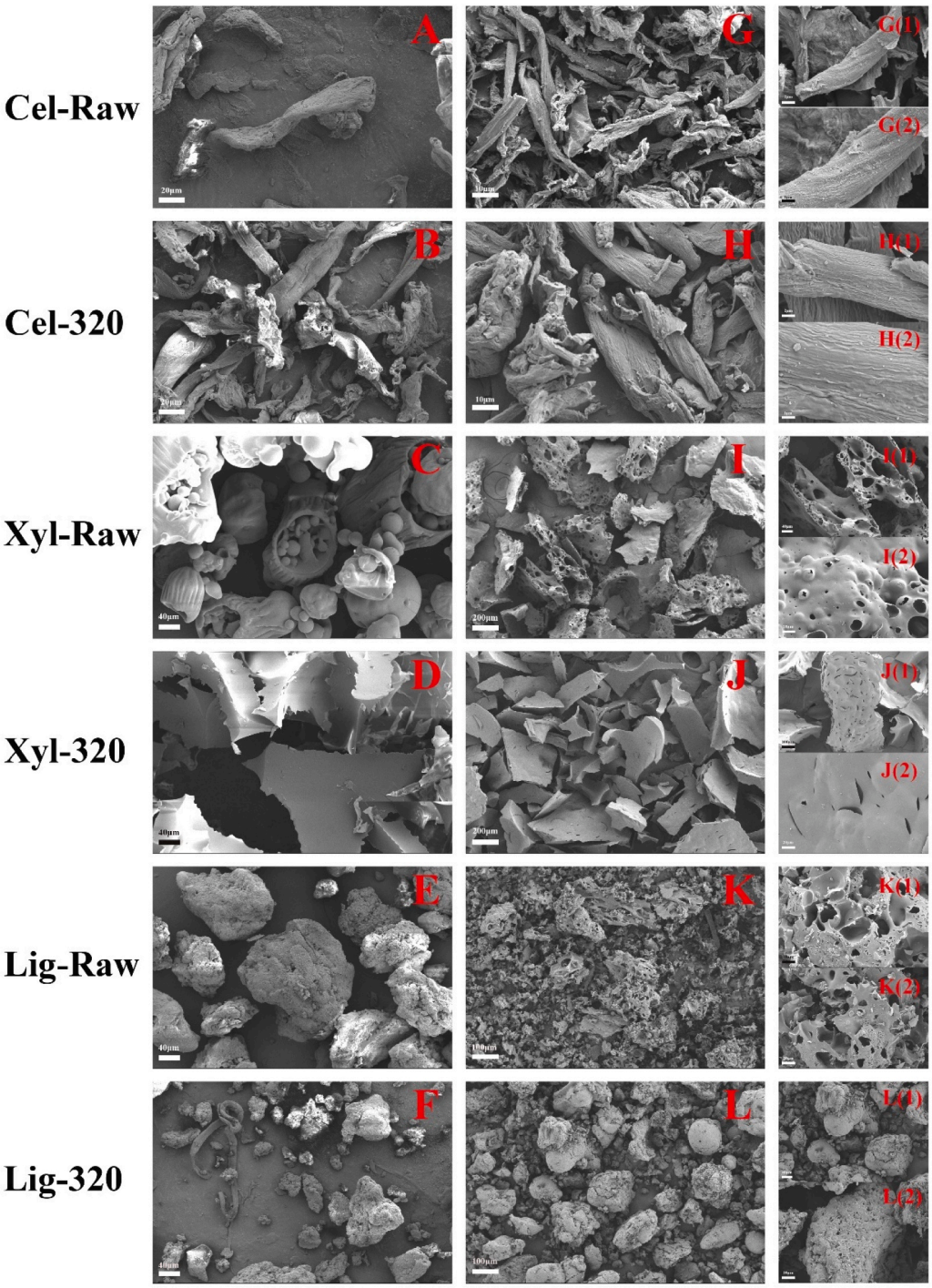

Fig. 8. SEM images of raw and torrefied three major constituents samples (A) Cel-Raw (B) Cel-320 (C) Xyl-Raw (D) Xyl-260 (E) Lig-Raw (F) Lig-200 and their chars (G) Cel-Raw char (H) Cel-320 char (I) Xyl-Raw char (J) Xyl-320 char (K) Lig-Raw char (L) Lig-320 char.

reaction during pyrolysis, which in turn enlarge the aromatic ring systems. Strong linear correlations between the band ratio A_D/A_{Ds} and accumulated char yield of cellulose, xylan and lignin can also be found in Fig. 10. This elucidated that the higher accumulated char yield of torrefied samples can be attributed to the larger aromatic systems enhanced by severer torrefaction.

4. Further discussion

Char formation during the pyrolysis of lignocellulosic biomass is influenced in a highly concerted manner by three intraparticle phenomena: mass transfer, chemical reactions, and phase change. Mass transfer of the volatiles out of the sample matrix after devolatilization plays a significant role in char formation. When the mass transport limitation in the solid matrix is enhanced, the trapped volatiles reacts further, promoting secondary reactions and increasing the char yield. Therefore, any factor that hinders mass transport increases charring [50, 51]. In addition, phase change, such as the formation of an intermediate "liquid-like" phase (also known as metaplast), also plays a critical role in the char formation by impacting both mass transfer and chemical reactions.

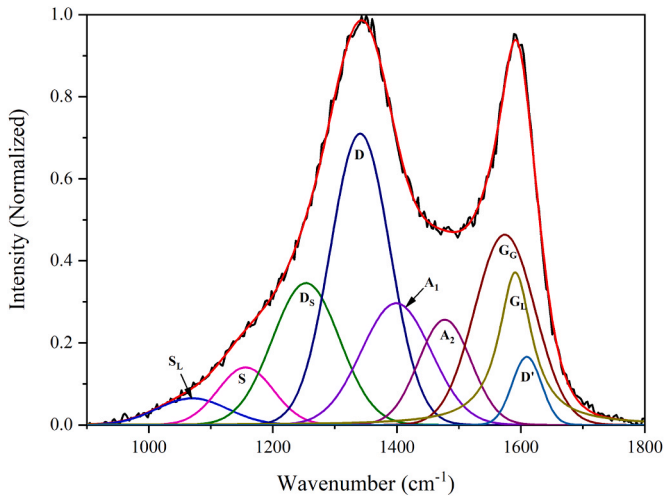

Fig. 9. A curve-fitted Raman spectrum of the char prepared from the fast pyrolysis of 200 °C-torrefied cellulose at 1028 °C.

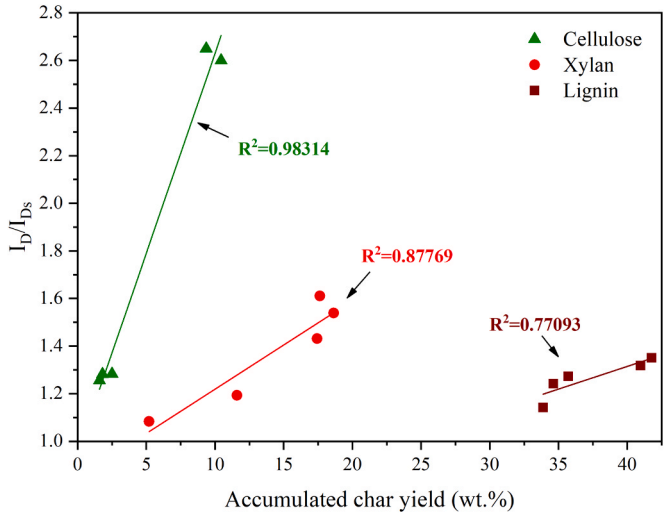

Fig. 10. Raman intensity ratios between D band and Ds bands of char prepared from raw and torrefied three major constituents.

4.1. Impact of torrefaction pretreatment on the char formation

It is a common observation that torrefaction pretreatment induces more or less intense chemical transformations within the polymers of lignocellulosic biomass. A combination of the results obtained by FTIR and ^{13}C NMR highlights the cleavage of the sidechain, the destruction of carbohydrate structure, and the formation of crosslinking structure for three constituent polymers observed by each method. The increase of the accumulated char yield by torrefaction pretreatment has been generally attributed to significant dehydration and crosslinking reactions that take place during torrefaction [52,53]. The crosslinking reactions that occurred during the torrefaction of constituent polymers are of major importance for charmakers as they can impact the three intraparticle phenomena during pyrolysis. The possible reason for increasing Y_c of the torrefied sample is that crosslinking structure forms during the earliest stages of pyrolysis (in the case of torrefaction pretreatment), then the thermal stability will be enhanced and the rate of metaplast crosslinking will be increased. The enhanced thermal stability and increasing rate of metaplast crosslinking favor cross-polymerization of the higher molecular weight fractions in the volatiles and finally promote char formation. This is plausible since the higher the molecular weight, the more potentially reactive crosslinking sites it contains [54].

Fig. 11 gives an overview of the mass fraction at different stages versus varying torrefaction severity for the three major biomass constituents. Notably, the values of both mass loss in torrefaction and accumulated char yield rise in tandem as torrefaction temperature increases, while the mass loss in pyrolysis decreases correspondingly. Thus, the second possibility of increasing the Y_c of the torrefied sample would be that devolatilization in torrefaction results in volatiles formed within the metaplast during pyrolysis cannot be released through the formation and rupture of bubbles on the particle surface because of insufficient pressure difference built up. Moreover, the bubbling process is necessary for thermal ejection, a crucial way to evacuate oligomers. The feeble bubbling process during pyrolysis caused by torrefaction pretreatment weakens the thermal ejection and therefore traps the oligomers. The trapped oligomers react further in the metaplast. Such secondary reactions of oligomeric products lead to higher char yields [55]. Enhancing transport limitation and promoting secondary reactions during pyrolysis caused by torrefaction increase the accumulated char yield. This possibility is supported by the SEM of the Xyl-320 char (Fig. 8J), as an example, which shows the smooth surface with less cavity and unbroken bubbles, implying insufficient pressure for volatiles escaping from the solid matrix during the thermoplastic phase.

4.2. Impact of pyrolysis heating rate on char formation

Heating rates play a crucial role in shaping the behavior of biomass pyrolysis, influencing the melting and bubbling processes, which, in turn, impact the competing mechanisms of char formation at different temperatures[56]. Mamleev et al.[57] highlighted that char formation predominantly occurs through secondary reactions in the liquid phase, where crosslinking and dehydration reactions, favorable for char formation, exhibit lower activation energy under low heating rates. At high heating rates, biomass experiences substantial bond-breaking before crosslinking takes place. Consequently, volatile is rapidly released through vigorous bubbling, resulting in shorter residence times and reduced secondary reactions, hence leading to a decrease in char yield. In essence, biomass pyrolysis follows distinct reaction pathways depending on the heating rate. It is commonly accepted that fast pyrolysis yields less char compared to slow pyrolysis, as evident in Fig. 6.

Char production is the most sensitive to heating rate variations. However, a notable observation in Fig. 6 is that torrefaction appears to mitigate the influence of heating rate, causing the accumulated char yield of fast pyrolysis to approach that of slow pyrolysis. This phenomenon can be attributed to the crosslinking and extensive release of volatiles during torrefaction, which restricts mass transfer and minimizes secondary reactions during fast pyrolysis. Thus, torrefaction pretreatment enables the samples to follow a reaction pathway toward char formation, which is similar to that of slow pyrolysis, and finally eliminating the disparity between fast and slow pyrolysis. Additionally, the comparable char yields of raw and torrefied components after slow pyrolysis may be attributed to the prolonged residence time at lower temperatures. This extended duration alters the composition of volatiles and reaction routes, promoting crosslinking. The crosslinking, occurring during the initial low-temperature stages of slow pyrolysis, leads to intraparticle phenomena during subsequent pyrolysis of raw samples that resemble those occurred during the pyrolysis of torrefied samples.

5. Conclusions

Thermal pretreatment has a profound effect on char yield and char reactivity. Our results indicate that the accumulated char yield is affected strongly by both torrefaction temperature and pyrolysis heating rate, which are mutually coupled. At the condition of fast pyrolysis, the torrefaction drastically increased the accumulated char yield of constituents, but the sensitivity of accumulated char yield to torrefaction temperature differed with varied constituents. Torrefaction also

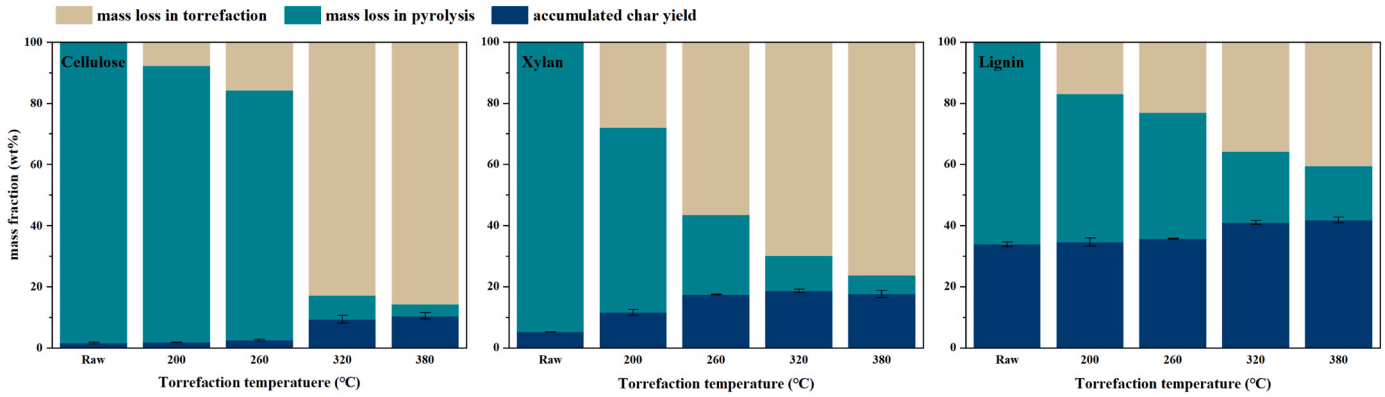

Fig. 11. Mass loss at different stages and accumulated char yield of the three major constituents torrefied at different temperatures.

presented a considerable effect on char oxidation reactivity, which resulted in a decrease in the char reactivities of cellulose and xylan, while its effect on lignin varied, with some torrefaction temperatures showing no effect and others showing promotion. The distribution of these biopolymers is a critical factor controlling char yield and char reactivity of torrefied biomass. The Raman spectra show a strong correlation between the relative amount of small and large aromatic rings and the accumulated char yield of torrefied samples. This suggests that the higher accumulated char yield in torrefied samples is due to the formation of large aromatic systems during torrefaction.

While the present study provides insights into the effect of torrefaction on char formation characteristics, there is still a need for a comprehensive understanding of the underlying mechanisms governing the influence of torrefaction on the charring process and char reactivity. Specifically, further investigation is warranted to explore the interplay between torrefaction and pyrolysis heating rate, which remains an area requiring deeper exploration.

CRediT authorship contribution statement

Jinzheng Chen: Investigation, Methodology, Data curation, Writing – original draft. **Zhimin Lu:** Conceptualization, Funding acquisition, Supervision, Writing – review and editing. **Jie Jian:** Conceptualization, Investigation, Methodology, Writing – review & editing. **Zhengyan Bao:** Writing – review & editing. **Jianfeng Cai:** Writing – review & editing. **Shunchun Yao:** Resource, Project administration.

Declaration of Competing Interest

The authors declare the following financial interests/personal relationships which may be considered as potential competing interests: Zhimin Lu reports financial support was provided by National Natural Science Foundation of China.

Data Availability

Data will be made available on request.

Acknowledgments

This work was supported by the National Natural Science Foundation of China (52276190), the Fundamental Research Funds for the Central Universities (2022ZFJH04) and the Nature Science Foundation of Guangdong Province (2022A1515010741).

Appendix A. Supporting information

Supplementary data associated with this article can be found in the online version at doi:10.1016/j.jaap.2023.106104.

References

[1] Y. Niu, Y. Lv, Y. Lei, S. Liu, Y. Liang, D. Wang, S. Hui, Biomass torrefaction: properties, applications, challenges, and economy, Renew. Sustain. Energy Rev. 115 (2019), 109395, https://doi.org/10.1016/j.rser.2019.109395.
[2] W.H. Chen, B.J. Lin, Y.Y. Lin, Y.S. Chu, A.T. Ubando, P.L. Show, H.C. Ong, J. S. Chang, S.H. Ho, A.B. Culaba, A. Pétrissans, M. Pétrissans, Progress in biomass torrefaction: principles, applications and challenges, Prog. Energy Combust. Sci. 82 (2021), https://doi.org/10.1016/j.pecs.2020.100887.
[3] S. Proskurina, J. Heinimö, F. Schipfer, E. Vakkilainen, Biomass for industrial applications: the role of torrefaction, Renew. Energy 111 (2017) 265–274, https://doi.org/10.1016/j.renene.2017.04.015.
[4] J.J. Chew, V. Doshi, Recent advances in biomass pretreatment - Torrefaction fundamentals and technology, Renew. Sustain. Energy Rev. 15 (2011) 4212–4222, https://doi.org/10.1016/j.rser.2011.09.017.
[5] M.J.C. van der Stelt, H. Gerhauser, J.H.A. Kiel, K.J. Ptasinski, Biomass upgrading by torrefaction for the production of biofuels: a review, Biomass-.-. Bioenergy 35 (2011) 3748–3762.
[6] Y.S. Chin, Impacts of Fuel Inventory on Low Temperature Ignition Risk during Handling and Storage of Biomass, (2017).
[7] B. Ru, S. Wang, G. Dai, L. Zhang, Effect of Torrefaction on Biomass Physicochemical Characteristics and the Resulting Pyrolysis Behavior, Energy Fuels 29 (2015) 5865–5874, https://doi.org/10.1021/acs.energyfuels.5b01263.
[8] A.C. Louwes, L. Basile, R. Yukananto, J.C. Bhagwandas, E.A. Bramer, G. Brem, Torrefied biomass as feed for fast pyrolysis: An experimental study and chain analysis, Biomass-.-. Bioenergy 105 (2017) 116–126, https://doi.org/10.1016/j.biombioe.2017.06.009.
[9] Z. Lu, J. Jian, P.A. Jensen, H. Wu, P. Glarborg, Influence of Torrefaction on single particle combustion of wood, Energy Fuels 30 (2016) 5772–5778, https://doi.org/10.1021/acs.energyfuels.6b00806.
[10] X. Li, Z. Lu, J. Chen, X. Chen, Y. Jiang, J. Jian, S. Yao, Effect of oxidative torrefaction on high temperature combustion process of wood sphere, Fuel 286 (2021), https://doi.org/10.1016/j.fuel.2020.119379.
[11] J. Jian, Z. Lu, S. Yao, Y. Li, Z. Liu, B. Lang, Z. Chen, Effects of thermal conditions on char yield and char reactivity of woody biomass in stepwise pyrolysis, J. Anal. Appl. Pyrolysis 138 (2019) 211–217, https://doi.org/10.1016/j.jaap.2018.12.026.
[12] J. Huang, Y. Qiao, H. Liu, B. Wang, Z. Wang, Y. Yu, M. Xu, Effect of torrefaction on physicochemical properties and steam gasification reactivity of chars produced from the pyrolysis of typical food wastes, Energy Fuels 34 (2020) 15332–15342, https://doi.org/10.1021/acs.energyfuels.0c03217.
[13] S. Xin, T. Mi, X. Liu, F. Huang, Effect of torrefaction on the pyrolysis characteristics of high moisture herbaceous residues, Energy 152 (2018) 586–593, https://doi.org/10.1016/j.energy.2018.03.104.
[14] R. Li, C. Wu, L. Zhu, Z. Hu, J. Xu, Y. Yang, F. Yang, Z. Ma, Regulation of the elemental distribution in biomass by the torrefaction pretreatment using different atmospheres and its influence on the subsequent pyrolysis behaviors, Fuel Process. Technol. 222 (2021), https://doi.org/10.1016/j.fuproc.2021.106983.
[15] S. Niksa, bio-FLASHCHAIN® theory for rapid devolatilization of biomass 2, Predict. Total yields Torre woods, Fuel 263 (2020), https://doi.org/10.1016/j.fuel.2019.116645.
[16] S. Niksa, bio-FLASHCHAIN® theory for rapid devolatilization of biomass 3, Predict. Total yields Torre grasses Agric. Residues, Fuel 263 (2020), https://doi.org/10.1016/j.fuel.2019.116646.
[17] P. McNamee, L.I. Darvell, J.M. Jones, A. Williams, The combustion characteristics of high-heating-rate chars from untreated and torrefied biomass fuels, Biomass-.-. Bioenergy 82 (2015) 63–72, https://doi.org/10.1016/j.biombioe.2015.05.016.
[18] Z. Lu, J. Jian, P. Arendt Jensen, H. Wu, P. Glarborg, Impact of KCl impregnation on single particle combustion of wood and torrefied wood, Fuel 206 (2017) 684–689, https://doi.org/10.1016/j.fuel.2017.05.082.
[19] L. Li, Y. Huang, D. Zhang, A. Zheng, Z. Zhao, M. Xia, H. Li, Uncovering Structure-Reactivity Relationships in Pyrolysis and Gasification of Biomass with Varying Severity of Torrefaction, ACS Sustain, Chem. Eng. 6 (2018) 6008–6017, https://doi.org/10.1021/acssuschemeng.7b04649.

[20] O. Karlström, M. Costa, A. Brink, M. Hupa, CO_2 gasification rates of char particles from torrefied pine shell, olive stones and straw, Fuel 158 (2015) 753–763, https://doi.org/10.1016/j.fuel.2015.06.011.
[21] D. Magalhães, K. Gürel, L. Matsakas, P. Christakopoulos, I. Pisano, J.J. Leahy, F. Kazanç, A. Trubetskaya, Prediction of yields and composition of char from fast pyrolysis of commercial lignocellulosic materials, organosolv fractionated and torrefied olive stones, Fuel 289 (2021), https://doi.org/10.1016/j.fuel.2020.119862.
[22] S. Zhang, Y. Su, Y. Xiong, H. Zhang, Physicochemical structure and reactivity of char from torrefied rice husk: effects of inorganic species and torrefaction temperature, Fuel 262 (2020), https://doi.org/10.1016/j.fuel.2019.116667.
[23] D. Chen, A. Gao, K. Cen, J. Zhang, X. Cao, Z. Ma, Investigation of biomass torrefaction based on three major components: hemicellulose, cellulose, and lignin, Energy Convers. Manag. 169 (2018) 228–237, https://doi.org/10.1016/j.enconman.2018.05.063.
[24] T. Melkior, S. Jacob, G. Gerbaud, S. Hediger, L. Le Pape, L. Bonnefois, M. Bardet, NMR analysis of the transformation of wood constituents by torrefaction, Fuel 92 (2012) 271–280, https://doi.org/10.1016/j.fuel.2011.06.042.
[25] J.L. Wen, S.L. Sun, T.Q. Yuan, F. Xu, R.C. Sun, Understanding the chemical and structural transformations of lignin macromolecule during torrefaction, Appl. Energy 121 (2014) 1–9, https://doi.org/10.1016/j.apenergy.2014.02.001.
[26] S. Wang, G. Dai, B. Ru, Y. Zhao, X. Wang, G. Xiao, Z. Luo, Influence of torrefaction on the characteristics and pyrolysis behavior of cellulose, Energy 120 (2017) 864–871, https://doi.org/10.1016/j.energy.2016.11.135.
[27] R. Mahadevan, S. Adhikari, R. Shakya, K. Wang, D.C. Dayton, M. Li, Y. Pu, A. J. Ragauskas, Effect of torrefaction temperature on lignin macromolecule and product distribution from HZSM-5 catalytic pyrolysis, J. Anal. Appl. Pyrolysis 122 (2016) 95–105, https://doi.org/10.1016/j.jaap.2016.10.011.
[28] A. Zheng, L. Jiang, Z. Zhao, Z. Huang, K. Zhao, G. Wei, X. Wang, F. He, H. Li, Impact of torrefaction on the chemical structure and catalytic fast pyrolysis behavior of hemicellulose, lignin, and cellulose, Energy Fuels 29 (2015) 8027–8034, https://doi.org/10.1021/acs.energyfuels.5b01765.
[29] Y. Haiping, Y. Rong, C. Hanping, H.L. Dong, Z. Chuguang, Characteristics of hemicellulose, cellulose and lignin pyrolysis, Fuel 86 (2007) 1781–1788.
[30] P. Lv, G. Almeida, P. Perré, TGA-FTIR analysis of torrefaction of lignocellulosic, BioResources 10 (2015) 4239–4251.
[31] P. Lv, G. Almeida, P. Perré, Torrefaction of cellulose: validity and limitation of the temperature/duration equivalence, BioResources 7 (2012) 3720–3731, https://doi.org/10.15376/biores.7.3.3720-3731.
[32] X. Cao, J. Zhang, K. Cen, F. Chen, D. Chen, Y. Li, Investigation of the relevance between thermal degradation behavior and physicochemical property of cellulose under different torrefaction severities, Biomass-.-. Bioenergy 148 (2021), 106061, https://doi.org/10.1016/j.biombioe.2021.106061.
[33] J. Liang, J. Chen, S. Wu, C. Liu, M. Lei, Comprehensive insights into xylan structure evolution via multi-perspective analysis during slow pyrolysis process, Fuel Process. Technol. 186 (2019) 1–7, https://doi.org/10.1016/j.fuproc.2018.12.014.
[34] H. Yang, S. Li, B. Liu, Y. Chen, J. Xiao, Z. Dong, M. Gong, H. Chen, Hemicellulose pyrolysis mechanism based on functional group evolutions by two-dimensional perturbation correlation infrared spectroscopy, Fuel 267 (2020), 117302, https://doi.org/10.1016/j.fuel.2020.117302.
[35] Y. Fan, L. Li, N. Tippayawong, S. Xia, F. Cao, X. Yang, A. Zheng, Z. Zhao, H. Li, Quantitative structure-reactivity relationships for pyrolysis and gasification of torrefied xylan, Energy 188 (2019), https://doi.org/10.1016/j.energy.2019.116119.
[36] G. Dai, Q. Zou, S. Wang, Y. Zhao, L. Zhu, Q. Huang, Effect of torrefaction on the structure and pyrolysis behavior of lignin, Energy Fuels 32 (2018) 4160–4166, https://doi.org/10.1021/acs.energyfuels.7b03038.
[37] Y.W. Chua, Y. Yu, H. Wu, Structural changes of chars produced from fast pyrolysis of lignin at 100–300 °C, Fuel (2019), https://doi.org/10.1016/j.fuel.2019.115754.
[38] R. El Hage, N. Brosse, L. Chrusciel, C. Sanchez, P. Sannigrahi, A. Ragauskas, Characterization of milled wood lignin and ethanol organosolv lignin from miscanthus, Polym. Degrad. Stab. 94 (2009) 1632–1638, https://doi.org/10.1016/j.polymdegradstab.2009.07.007.
[39] N. Brosse, R. El Hage, M. Chaouch, M. Pétrissans, S. Dumarçay, P. Gérardin, Investigation of the chemical modifications of beech wood lignin during heat treatment, Polym. Degrad. Stab. 95 (2010) 1721–1726, https://doi.org/10.1016/j.polymdegradstab.2010.05.018.
[40] J. Yu, N. Paterson, J. Blamey, M. Millan, Cellulose, xylan and lignin interactions during pyrolysis of lignocellulosic biomass, Fuel 191 (2017) 140–149, https://doi.org/10.1016/j.fuel.2016.11.057.
[41] A. Trubetskaya, M.T. Timko, K. Umeki, Prediction of fast pyrolysis products yields using lignocellulosic compounds and ash contents, Appl. Energy 257 (2020), 113897, https://doi.org/10.1016/j.apenergy.2019.113897.
[42] E.M. Fisher, C. Dupont, L.I. Darvell, J.M. Commandré, A. Saddawi, J.M. Jones, M. Grateau, T. Nocquet, S. Salvador, Combustion and gasification characteristics of chars from raw and torrefied biomass, Bioresour. Technol. 119 (2012) 157–165, https://doi.org/10.1016/j.biortech.2012.05.109.
[43] T. Li, M. Geier, L. Wang, X. Ku, B.M. Güell, T. Løvås, C.R. Shaddix, Effect of torrefaction on physical properties and conversion behavior of high heating rate char of forest residue, Energy Fuels 29 (2015) 177–184, https://doi.org/10.1021/ef5016044.
[44] Y. Zhang, P. Geng, R. Liu, Synergistic combination of biomass torrefaction and co-gasification: 1. React. Stud., Bioresour. Technol. 245 (2017) 225–233, https://doi.org/10.1016/j.biortech.2017.08.197.
[45] M.W. Smith, B. Pecha, G. Helms, L. Scudiero, M. Garcia-Perez, Chemical and morphological evaluation of chars produced from primary biomass constituents: Cellulose, xylan, and lignin, Biomass-. Bioenergy 104 (2017) 17–35, https://doi.org/10.1016/j.biombioe.2017.05.015.
[46] D. Zhong, Z. Chang, K. Zeng, J. Li, Y. Qiu, Q. Lu, G. Flamant, H. Yang, H. Chen, Solar pyrolysis of biomass - part II: the physicochemical structure evolution of char, Fuel 333 (2023), 126474, https://doi.org/10.1016/j.fuel.2022.126474.
[47] S. Wu, S. Huang, L. Ji, Y. Wu, J. Gao, Structure characteristics and gasification activity of residual carbon from entrained-flow coal gasification slag, Fuel 122 (2014) 67–75, https://doi.org/10.1016/j.fuel.2014.01.011.
[48] A. Zaida, E. Bar-Ziv, L.R. Radovic, Y.J. Lee, Further development of Raman Microprobe spectroscopy for characterization of char reactivity, Proc. Combust. Inst. 31 II (2007) 1881–1887. https://doi.org/10.1016/j.proci.2006.07.011.
[49] M.W. Smith, I. Dallmeyer, T.J. Johnson, C.S. Brauer, J.S. McEwen, J.F. Espinal, M. Garcia-Perez, Structural analysis of char by Raman spectroscopy: improving band assignments through computational calculations from first principles, Carbon N. Y 100 (2016) 678–692, https://doi.org/10.1016/j.carbon.2016.01.031.
[50] I. Milosavljevic, V. Oja, E.M. Suuberg, Thermal effects in cellulose pyrolysis: relationship to char formation processes, Ind. Eng. Chem. Res. 35 (1996) 653–662, https://doi.org/10.1021/ie950438l.
[51] J.L. Banyasz, S. Li, J.L. Lyons-Hart, K.H. Shafer, Cellulose pyrolysis: the kinetics of hydroxyacetaldehyde evolution, J. Anal. Appl. Pyrolysis 57 (2001) 223–248, https://doi.org/10.1016/S0165-2370(00)00135-2.
[52] S. Zhang, B. Hu, L. Zhang, Y. Xiong, Effects of torrefaction on yield and quality of pyrolysis char and its application on preparation of activated carbon, J. Anal. Appl. Pyrolysis 119 (2016) 217–223, https://doi.org/10.1016/j.jaap.2016.03.002.
[53] P. Guo, W.L. Saw, P.J. Van Eyk, E.B. Stechel, R. De Nys, P.J. Ashman, G.J. Nathan, Gasification Reactivity and Physicochemical Properties of the Chars from Raw and Torrefied Wood, Grape Marc, and Macroalgae, Energy Fuels 31 (2017) 2246–2259, https://doi.org/10.1021/acs.energyfuels.6b02215.
[54] Peter R. Solomon, Michael A. Serio, Eric M. Suuberg, Coal pyrolysis: experiments, kinetic rates and mechanisms, Prog. Energy Combust. Sci. 18 (1992) 133–220.
[55] J. Montoya, B. Pecha, F.C. Janna, M. Garcia-Perez, Single particle model for biomass pyrolysis with bubble formation dynamics inside the liquid intermediate and its contribution to aerosol formation by thermal ejection, J. Anal. Appl. Pyrolysis 124 (2017) 204–218, https://doi.org/10.1016/j.jaap.2017.02.004.
[56] A. Trubetskaya, Fast Pyrolysis of Biomass at High Temperatures, Technical University of Denmark, 2016.
[57] V. Mamleev, S. Bourbigot, M. Le Bras, J. Yvon, The facts and hypotheses relating to the phenomenological model of cellulose pyrolysis. Interdependence of the steps, J. Anal. Appl. Pyrolysis 84 (2009) 1–17, https://doi.org/10.1016/j.jaap.2008.10.014.